Observation of Kink Instability as Driver of Recurrent Flares in AR 10960

A.K. Srivastava*

Aryabhatta Research Institute of Observational Sciences (ARIES), Manora Peak, Nainital-263 129, India.
**E-mail: aks@aries.res.in*

Pankaj Kumar

Aryabhatta Research Institute of Observational Sciences (ARIES), Manora Peak, Nainital-263 129, India.

T.V. Zaqarashvili

Space Research Institute, Austrian Academy of Sciences, Graz 8042, Austria.

Abastumani Astrophysical Observatory at Ilia State University, Al Kazbegi ave. 2a, 0160 Tbilisi, Georgia.

B.P. Filippov

Pushkov Institute of Terrestrial Magnetism, Ionosphere and Radio Wave Propagation, Russian Academy of Sciences, Troitsk Moscow Region 142190, Russia.

M.L. Khodachenko

Space Research Institute, Austrian Academy of Sciences, Graz 8042, Austria.

Wahab Uddin

Aryabhatta Research Institute of Observational Sciences (ARIES), Manora Peak, Nainital-263 129, India.

We study the active region NOAA 10960, which produces two flare events (B5.0, M8.9) on 04 June 2007. We find the observational signature of right handed helical twists in the loop system associated with this active region. The first B5.0 flare starts with the activation of helical twist showing ∼3 turns. However, after ∼20 minutes another helical twist (with ∼2 turns) appears, which triggers M8.9 flare. Both helical structures were closely associated with a small positive polarity sunspot in the AR. We interpret these observations as evidence of kink instability, which triggers the recurrent solar flares.

1. Introduction

Solar flares are transient explosions in the solar atmosphere when the energy of stressed and twisted magnetic fields is released into heating and radiation. The flares associated with coronal mass ejections (CME) are known as "eruptive flares", while flares without CMEs are known as "confined flares". The large flares accompanied with energetic CMEs may be triggered by flux-rope eruption with significant changes in the photospheric fields [1,2]. The flares can also be initiated due to the filament interactions followed by halo CMEs [3 and references cited there] and filament eruptions [4 and references cited there]. Observations show that the moderate flares without CME may be triggered by some instabilities (e.g., kink instability) [5,6]. The instabilities may cause the destabilization of large-scale magnetic field, and can result CMEs [7 and references cited there]. Instability of twisted magnetic flux tubes are well studied in theory and intense numerical simulations [8–10].

Kumar et al. [6] have recently presented a detailed multi-wavelength observations of the M8.9/3B class solar flare in the active region NOAA 10960 on 04 June 2007. They concluded that the positive flux emergence, the penumbral filament loss of the associated sunspot and the activation of the several twisted flux ropes in and around the flare site can be key candidates for the occurrence of this flare during 05:06 UT and 05:13 UT. The "activation" implies motion/brightening in the flux rope which is generated by some instability. A small B5.0 class flare has also been observed in the same active region during 04:40-04:51 UT, which seems to be a precursor for the M8.9 flare [5]. These two recurrent flares have been occurred during the activation of successive helical twist and kink unstable flux tubes from a positive polarity sunspot of AR 10960 [5,6].

In this paper, we review the occurrence of recurrent solar flares and associated multi-wavelength phenomena. Multi-wavelength observations are described in section 2. The observational results are presented in section 3. The discussion and conclusions are given in the last section.

2. Observational Data Sets

SOHO MDI data: We use the SOHO/MDI data in order to show the magnetic structure of the active region [11]. The cadence of images is 96 minute and the pixel resolution is $1.98''$.

TRACE data: We use TRACE 171 Å (Fe IX) EUV images to study the dynamics of the flaring active region and its response in the corona during

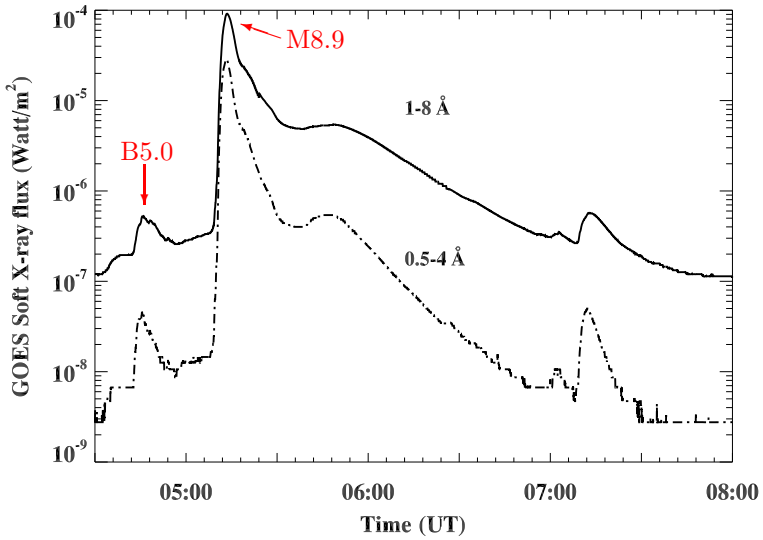

Fig. 1. GOES Soft X-ray flux profiles in two different wavelength bands for both flares (indicated by arrows) on 4 June 2007.

the flare event [12]. This wavelength corresponds to 1.3 MK plasma. The image size is 1024×1024 pixels with resolution of 0.5″ per pixel, and the cadence is ∼one minute. We have used the standard IDL routines available in the SolarSoft library for cleaning and co-aligning the images.

Hinode SOT and XRT data: We use Hindoe SOT G-band and Ca II H line data to study the photospheric and chromospheric responses with an angular resolution of 0.25 arcseconds, or 175 km over the field of view of about 400″×400″ on the Sun [13]. For coronal study of the event, we use Hinode XRT data with an angular resolution of about 2″ over a broad temperature range of 1–30 MK with full disk and a temporal resolution as short as 2 s [14].

STEREO SECCHI data: For the impulsive phase of the flare, we use the STEREO-A/SECCHI/EUVI observations [15]. We use Fe IX 171 Å coronal images for the present study. The size of each image is 2048×2048 pixels with 1.6″ per pixel sampling. We use the standard SECCHI_PREP subroutines for cleaning the images and other standard subroutines available in STEREO package SolarSoft library.

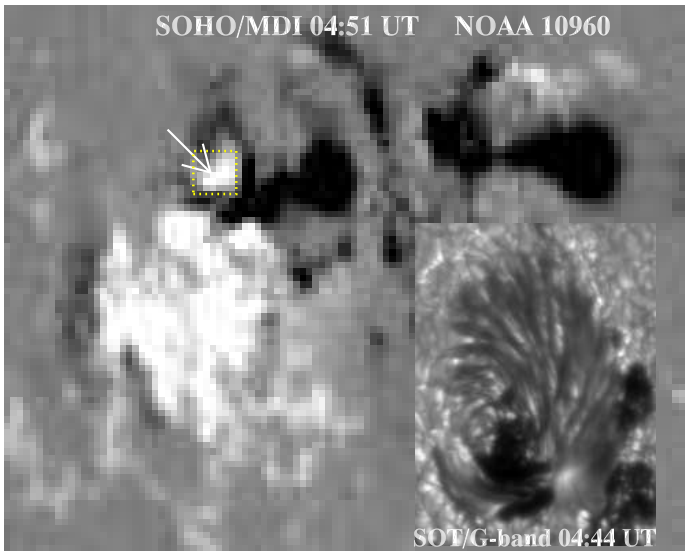

Fig. 2. SOHO/MDI magnetogram of the active region NOAA 10960 on 4 June 2007. The small positive polarity sunspot is shown in the box, indicated by an arrow. The enlarged view of the same sunspot is shown in Hinode SOT/G-band image in the bottom-right corner.

3. Observational Results

Figure 1 displays the GOES Soft X-ray flux profile in two wavelength bands (1–8 and 0.5–4 Å). Both flares (B5.0 and M8.9) are indicated by arrows. According to this profile, first B5.0 flare starts at 04:40 UT , attains maximum at 04:43 UT and ended at 04:51 UT. Another M8.9 flare starts at 05:06 UT, maximizes at 05:13 and ended at ∼05:30 UT. In Hα classification, this flare was long duration event classified as 3B, which starts at 05:05 UT and ends at 06:42 UT. Figure 2 shows the complex active region (AR) NOAA 10960 in SOHO MDI image with $\beta\gamma\delta$ magnetic configuration. This AR was very poor in CME production and only two M-class flares were associated with CMEs [16]. The small positive polarity sunspot shown in the box, indicated by an arrow plays the crucial role in triggering recurrent flare activities in the AR. The enlarged view of the same sunspot is shown in Hinode SOT/G-band image in the bottom-right corner. Twisted helical structures were activated above this sunspot during the initiation of both flares. The enlarged view of this sunspot is shown in SOT/G-band image in the bottom-right corner of this image. The sunspot shows highly twisted penumbral filaments oriented in the counter-clockwise direction.

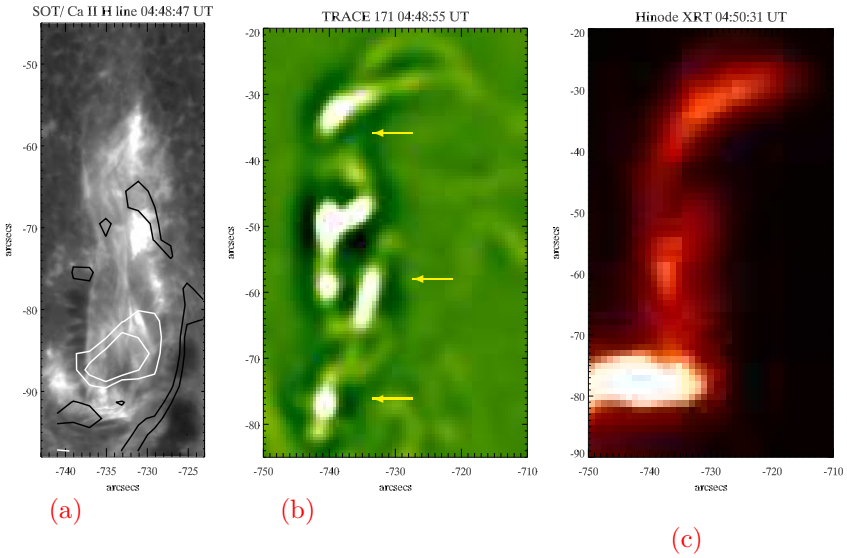

Fig. 3. (a) Hinode SOT/Ca II H line image showing the chromospheric part of first helical twisted magnetic structure during the first B5.0 flare. SOHO MDI contours overlaid on this image shows that the twist activation is associated with small positive polarity sunspot (white=positive polarity, black=negative polarity). (b) TRACE 171 Å EUV wavelet filtered image showing ∼3 turns (indicated by yellow arrows) in the helical twisted structure. (c) Hinode/XRT image showing the twisted structure during B5.0 flare.

The left-most panel of Figure 3 shows the chromospheric part of first helical twisted magnetic structure above the positive polarity sunspot during the B5.0 class solar flare at 04:48 UT. The MDI/SOHO contours are over-plotted on the Ca II H 3968 Å Hinode/SOT image. The white contours show the positive magnetic polarity, while the black contours show the negative magnetic polarity. The middle panel shows TRACE 171 Å EUV wavelet filtered image on the same time, which shows the $\sim$ 3 turns of the helical twist above the same positive polarity sunspot in the corona. Therefore, the total twist angle, $\Phi \sim 6.0\pi$ is much larger than the Kruskal -Shafranov instability criterion ($\Phi > 2.5\pi$) for the generation of the kink instability. The XRT images co-aligned with the TRACE, is presented in the right-most panel of Figure 3. Sudden brightening and enhancement of soft X-ray flux in the loop has also been evident around 04:49-04:50 UT by XRT/Hinode. The loop is twisted during the full span of the B5.0 flare duration, however, the twist maximizes with the flare around ∼04:48–04:49 UT. The right-handed (positive) twist is also clearly visible at 04:50 UT in

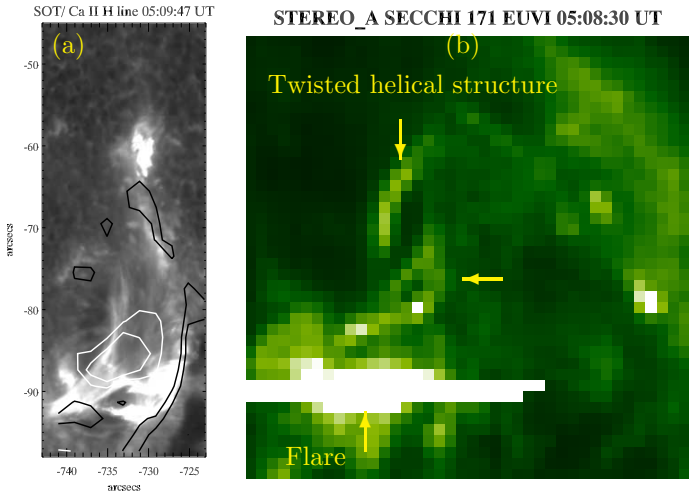

Fig. 4. (a) Hinode SOT/Ca II H line image showing the chromospheric part of second helical twisted magnetic structure during the second 3B/M8.9 flare. SOHO MDI contours overlaid on this image shows that the twist activation is associated with small positive polarity sunspot (white=positive polarity, black=negative polarity). (b)(b) STEREO A SECCHI 171 Å EUV image showing ∼2 turns in the helical twisted structure during M8.9 flare. The size of this image is $40\times40''$.

the XRT temporal image, which confirms the nature of twist as visible in the EUV 171 Å image from TRACE. The double structure of loop top in 171 Å is also visible during the flare event.

The left panel of Figure 4 shows the chromospheric part of second helical twisted magnetic structure above the same positive polarity sunspot during the M8.9/3B class solar flare at 05:09 UT. The MDI/SOHO contours are over-plotted on the Ca II H 3968 Å Hinode/SOT image. The white contours show the positive magnetic polarity, while the black contours show the negative magnetic polarity. It is clearly evident that M-class flare initiated above the same positive polarity sunspot, where the B-class flare occurred. The right panel shows STEREO-A/SECCHI EUVI 171 Å image, which shows nearly ∼2 turns indicated by arrows in the second activation of the helical twist on the same time above the positive polarity sunspot in the corona. Therefore, the total twist angle, $\Phi \sim 4.0\pi$ is still much larger than the Kruskal -Shafranov instability criterion. On the other hand, TRACE has no observations during the impulsive phase of the M8.9/3B flare.

Figure 5 (Top panel) shows the Nobeyama Radiheliograph (NoRH) 17 GHz contours overlaid on the SOHO/MDI image. It shows the two radio

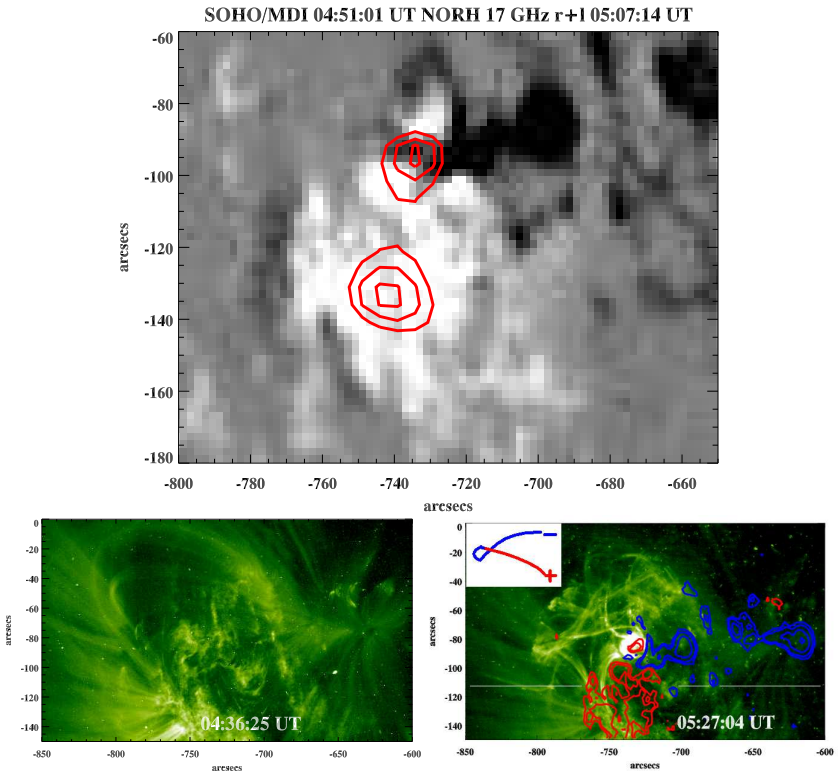

Fig. 5. Top: Nobeyama Radioheliograph (NoRH) 17 GHz contours overlaid on MDI image on 4 June 2007. Bottom: TRACE 171 Å EUV images showing the magnetic field environment in the AR before the flare (left panel) and during the decay phase of the flare (right panel).

sources. One radio source is located close to small positive polarity sunspot where the activation of helical twists takes place, whereas another source is located at the center of major positive polarity sunspot region. Bottom panels of Figure 5 shows the TRACE 171 Å EUV images before the recurrent flares (04:36 UT, left panel) and during the decay phase of the M-class flare (05:27 UT, right panel). The left image shows a well organized loop-system in the AR connecting opposite polarity regions. The right image shows the SOHO/MDI contours overlaid on TRACE 171 Å image Red=positive, Blue=negative). The careful study of this image reveals the activation of flux rope above the small positive polarity sunspot, which is evident in the earlier high resolution observations of this event (refer to Figures 3 and 4). The right footpoint of the flux rope seems to be anchored in the negative

polarity field region. The knot (kink) structure and the morphology of the flux rope is shown in the top-left corner of this image.

4. Discussion and Conclusions

We study the recurrent flare activities in the active region NOAA AR 10960, which are accompanied by activations of helical twists over the small positive polarity δ sunspot.

Srivastava et al. [5] have observed the first activation of a highly (right-handed) twisted flux tube in AR 10960 during the period 04:43–04:52 UT. They have estimated the length and the radius of the loop as L$\sim$80 Mm and a$\sim$4.0 Mm respectively, and also estimated the total maximum twist angle as $\sim 12\pi$, by assuming quasi-symmetric distribution of the twist along the magnetic loop, which is much larger than the Kruskal–Shafranov instability criterion. They suggested that the right-handed twist is symmetrically distributed along the observed loop as a possible asymmetry can be smoothed over the short Alfvén time of $\sim$80 s. The detection of a clear double structure of the loop top during 04:47–04:51 UT in TRACE 171 Å images are found to be consistent with simulated kink instability in curved coronal loops (Török et al. [8]. They have suggested that the kink instability of this twisted magnetic loop triggered the B5.0 class solar flare, which occurred during 04:40 –04:51 UT in this active region. The co-spatial brightening in soft X-rays as observed by Hinode/XRT and the co-temporal occurrence of the right-handed twisting in the flux tube confirm the occurrence of the B5.0 flare during 04:40–04:51 UT probably due to the generation of the kink instability.

Kumar et al. [6] have found multi-wavelength evidence of the successive activation of helical twists that may help in the energy build-up process at the flaring region in AR10960. The energy is released in the form of M-class flare after secondary activation of helical twist in the flux tube when it reconnects with neighboring opposite field. The activation of two helical structures/ropes played an important role in destabilizing and consecutive reconnection of magnetic field. The twist in the secondary magnetic structure crosses the threshold (2.5–3.5π), which probably produces the kink instability in this structure. The energy release region in the M-class flare coincides with the twisted magnetic structures. The M-class flare showed agreement with the quadrupolar (closed–closed) reconnection model (breakout) between two closed field lines [17], which is evident in the decay phase of this flare (see bottom-right panel of Figure 5 also). The asymmetric evolution is driven by foot-point shearing of one side of an arcade, where

reconnection between the sheared arcade and the neighboring (unsheared) flux system most probably triggers the flare. The kink instable twisted magnetic structure may undergo in a weak reconnection with the surrounding closed field lines in quadrupolar field configuration. Therefore, it triggers M-class flare in the active region without any eruption/CME [18–20].

Disappearance of Penumbrae during the decay phase and after the flare suggests that the magnetic field changes from inclined to almost vertical configuration [6]. This means that the part of penumbral magnetic field is converted into umbral fields. These results are in agreement with previous studies [21,22]. The rotation of sunspot was the most plausible cause of the helical twist and thus energy release in B5.0 class flare [5]. On the other hand, the penumbral loss and umbral area enhancement were clearly evident during M-class flare [6].

Nobeyama 17 GHz radio contours overlaid the SoHO/MDI image during the M-class flare show the two radio sources, corresponding to the footpoints of magnetic loop system, which are generated during the impulsive phase of the M-class flare due to particle acceleration from the reconnection site. The bottom-right panel of Figure 5 shows the TRACE 171 Å image in which the same bright loop system is clearly evident in the southward direction. The part of rising helical structure most likely reconnects with the southward loop-system and produce two radio sources due to particle acceleration from the reconnection site. These radio sources are the footpoints of the flaring loop system. The existence of co-spatial radio sources with this loop-system suggests the reconnection of twisted flux rope with the ambient field as most possible scenario for the flare triggering [6].

In conclusions, this paper reviews the rare observational signature of kink instability associated with failed eruptions and solar flares. Earlier, several researchers have been reported kink instability associated with CME eruptions [4,7 and references cited there]. The very interesting active region AR10960 was poor CME generator, but triggered many solar flares during its journey over the solar-disk. The multi-wavelength signature of helically twisted structures has been found as the cause of the recurrent solar flares on 04 June 2007. Therefore, we suggest that such flares may occur due to some instability/activation of twisted magnetic fields. The detailed multi-wavelength and statistical studies should be performed in future with the high- resolution space borne and ground-based observations.

Acknowledgments

We thank to the reviewers for their constructive suggestions. We are thankful for the data from different space-based instruments i.e. SOHO, GOES. SOHO is a project of international cooperation between ESA and NASA. The radio data from Nobeyama is thankfully acknowledged. This work was supported by the Department of Science and Technology, Ministry of Science and Technology of India, by the Russian foundation for Basic Research (grants 09-02-00080 and 09-02-92626, INT/RFBR/P-38) and by the Austrian Fond zur Förderung der Wissenschaftlichen Forschung (project P21197-N16). The work of T.Z was also supported by the Georgian National Science Foundation grant GNSF/ST09/4-310.

References

1. G. A. Gary and R. L. Moore, *ApJ* **611**, 545(August 2004).
2. Y. Liu, Y. Jiang, H. Ji, H. Zhang and H. Wang, *Astrophys. J.* **593**, L137(August 2003).
3. P. Kumar, P. K. Manoharan and W. Uddin, *ApJ* **710**, 1195(February 2010).
4. R. Liu, H. R. Gilbert, D. Alexander and Y. Su, *ApJ* **680**, 1508(June 2008).
5. A. K. Srivastava, T. V. Zaqarashvili, P. Kumar and M. L. Khodachenko, *ApJ* **715**, 292(May 2010).
6. P. Kumar, A. K. Srivastava, B. Filippov and W. Uddin, *Sol. Phys.* **266**, 39(September 2010).
7. K. Cho, J. Lee, S. Bong, Y. Kim, B. Joshi and Y. Park, *ApJ* **703**, 1(September 2009).
8. T. Török, B. Kliem and V. S. Titov, *Astron. Astroph.* **413**, L27(January 2004).
9. T. Török and B. Kliem, *Astrophys. J.* **630**, L97(September 2005).
10. M. Haynes and T. D. Arber, *Astron. Astroph.* **467**, 327(May 2007).
11. P. H. Scherrer, R. S. Bogart, R. I. Bush, J. T. Hoeksema, A. G. Kosovichev, J. Schou, W. Rosenberg, L. Springer, T. D. Tarbell, A. Title, C. J. Wolfson, I. Zayer and MDI Engineering Team, *Sol. Phys.* **162**, 129(December 1995).
12. B. N. Handy, L. W. Acton, C. C. Kankelborg, C. J. Wolfson, D. J. Akin, M. E. Bruner, R. Caravalho, R. C. Catura, R. Chevalier, D. W. Duncan, C. G. Edwards, C. N. Feinstein, S. L. Freeland, F. M. Friedlaender, C. H. Hoffmann, N. E. Hurlburt, B. K. Jurcevich, N. L. Katz, G. A. Kelly, J. R. Lemen, M. Levay, R. W. Lindgren, D. P. Mathur, S. B. Meyer, S. J. Morrison, M. D. Morrison, R. W. Nightingale, T. P. Pope, R. A. Rehse, C. J. Schrijver, R. A. Shine, L. Shing, K. T. Strong, T. D. Tarbell, A. M. Title, D. D. Torgerson, L. Golub, J. A. Bookbinder, D. Caldwell, P. N. Cheimets, W. N. Davis, E. E. Deluca, R. A. McMullen, H. P. Warren, D. Amato, R. Fisher, H. Maldonado and C. Parkinson, *Sol. Phys.* **187**, 229(July 1999).
13. S. Tsuneta, K. Ichimoto, Y. Katsukawa, S. Nagata, M. Otsubo, T. Shimizu, Y. Suematsu, M. Nakagiri, M. Noguchi, T. Tarbell, A. Title, R. Shine,

W. Rosenberg, C. Hoffmann, B. Jurcevich, G. Kushner, M. Levay, B. Lites, D. Elmore, T. Matsushita, N. Kawaguchi, H. Saito, I. Mikami, L. D. Hill and J. K. Owens, *Sol. Phys.* **249**, 167(June 2008).

14. L. Golub, E. Deluca, G. Austin, J. Bookbinder, D. Caldwell, P. Cheimets, J. Cirtain, M. Cosmo, P. Reid, A. Sette, M. Weber, T. Sakao, R. Kano, K. Shibasaki, H. Hara, S. Tsuneta, K. Kumagai, T. Tamura, M. Shimojo, J. McCracken, J. Carpenter, H. Haight, R. Siler, E. Wright, J. Tucker, H. Rutledge, M. Barbera, G. Peres and S. Varisco, *Sol. Phys.* **243**, 63(June 2007).
15. J. Wuelser, J. R. Lemen, T. D. Tarbell, C. J. Wolfson, J. C. Cannon, B. A. Carpenter, D. W. Duncan, G. S. Gradwohl, S. B. Meyer, A. S. Moore, R. L. Navarro, J. D. Pearson, G. R. Rossi, L. A. Springer, R. A. Howard, J. D. Moses, J. S. Newmark, J. Delaboudiniere, G. E. Artzner, F. Auchere, M. Bougnet, P. Bouyries, F. Bridou, J. Clotaire, G. Colas, F. Delmotte, A. Jerome, M. Lamare, R. Mercier, M. Mullot, M. Ravet, X. Song, V. Bothmer and W. Deutsch, EUVI: the STEREO-SECCHI extreme ultraviolet imager, in *Society of Photo-Optical Instrumentation Engineers (SPIE) Conference Series*, ed. S. Fineschi & M. A. Gummin, Presented at the Society of Photo-Optical Instrumentation Engineers (SPIE) Conference, Vol. 5171February 2004.
16. S. Yashiro, N. Gopalswamy and S. Akiyama, *AGU Spring Meeting Abstracts* , A3+(May 2008).
17. S. K. Antiochos, *Astrophys. J.* **502**, L181+(August 1998).
18. S. K. Antiochos, C. R. DeVore and J. A. Klimchuk, *ApJ* **510**, 485(January 1999).
19. G. Aulanier, E. E. DeLuca, S. K. Antiochos, R. A. McMullen and L. Golub, *ApJ* **540**, 1126(September 2000).
20. M. J. Aschwanden, *Physics of the Solar Corona. An Introduction* (Praxis Publishing Ltd, August 2004).
21. H. Wang, C. Liu, J. Qiu, N. Deng, P. R. Goode and C. Denker, *Astrophys. J.* **601**, L195(February 2004).
22. C. Liu, N. Deng, Y. Liu, D. Falconer, P. R. Goode, C. Denker and H. Wang, *ApJ* **622**, 722(March 2005).

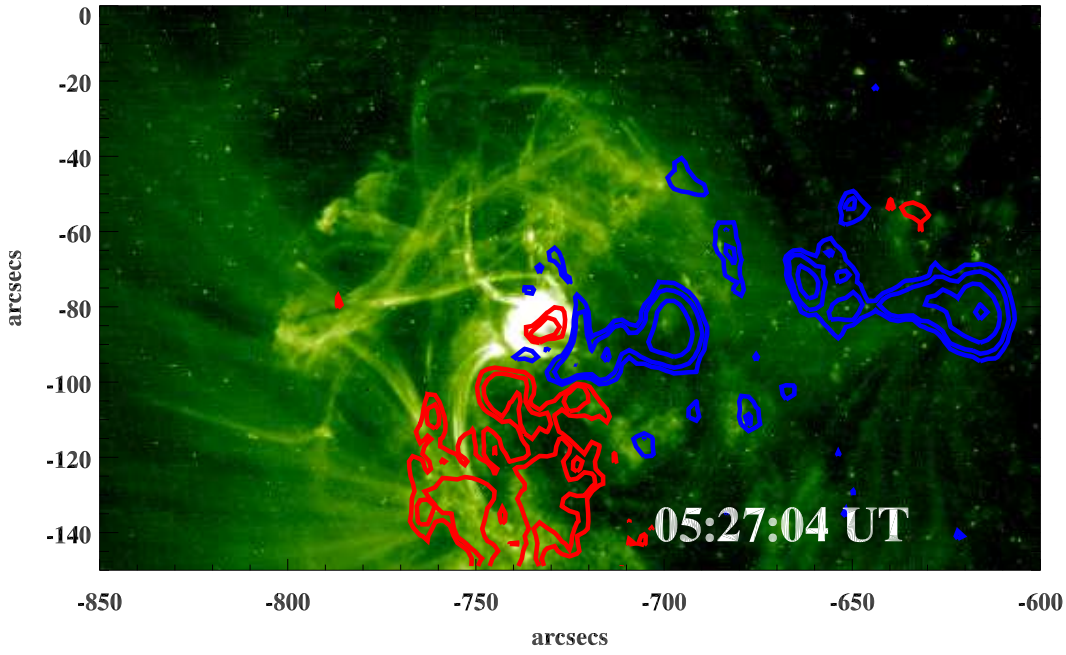
0
-20
-40
-60
-80
-100
-120
-140
arcsecs
-850
-800
-750
-700
-650
-600
arcsecs
05:27:04 UT